

A Survey for Young Spectroscopic Binary K7–M4 Stars in Ophiuchus

L. PRATO¹

ABSTRACT

This paper describes a high-resolution, infrared spectroscopic survey of young, low-mass stars designed to identify and characterize pre–main-sequence spectroscopic binaries. This is the first large infrared radial velocity survey of very young stars to date. The frequency and mass ratio distribution of the closest, low-mass binaries bear directly on models of stellar, brown dwarf, and planetary mass companion formation. Furthermore, spectroscopic binaries can provide mass ratios and ultimately masses, independent of assumptions, needed to calibrate models of young star evolution. I present the initial results from observations of a uniform sample of 33 T Tauri M stars in the Ophiuchus molecular cloud. The average mass of this sample is less than that of other young star radial velocity surveys of similar scope by a factor of ~ 2 . Almost every star was observed at 3–4 epochs over 3 years with the 10 meter Keck II telescope and the facility infrared spectrometer NIRSPEC. An internal precision of 0.43 km s^{-1} was obtained with standard cross-correlation calibration techniques. Four of the targets are newly discovered spectroscopic binaries, one of which is located in a sub-arcsecond, hierarchical quadruple system. Three other sub-arcsecond visual binaries were also serendipitously identified during target acquisition. The spectroscopic multiplicity of the sample is comparable to that of earlier type, pre–main-sequence objects. Therefore, there is no dearth of young, low-mass spectroscopic binary stars, at least in the Ophiuchus region.

Subject headings: binaries: spectroscopic — binaries: visual — stars: low-mass — stars: pre-main sequence — techniques: radial velocities — techniques: spectroscopic

1. Introduction

The ratio of binary to single stars on main-sequence is known to vary as a function of spectral type (Abt 1983). In some star forming regions (SFRs), this ratio is known to be

¹Lowell Observatory, 1400 West Mars Hill Rd. Flagstaff, AZ 86001; lprato@lowell.edu

in excess of the field star binary frequency (Duquennoy & Mayor 1991), however, in other SFRs, it is the same as that of the field stars. Siegler et al. (2003, 2005) and Burgasser et al. (2003) find evidence for a decreasing wide binary frequency associated with very low-mass stars and brown dwarfs in the field. Binary frequency appears to also be a function of the mass ratio, as illustrated, for example, by the differences in the numbers of stellar versus substellar companions to G stars (e.g., Duquennoy & Mayor 1991; Mazeh et al. 1992; Marcy & Butler 2000). As searches for binary systems have become more complete, the observational findings create ever more stringent conditions that must be accounted for in any uniform model of star, brown dwarf, and planet formation. However, because the extent of dynamical evolution is an open question, the most useful observations for constraining binary formation models are those based on the youngest observable stars.

Multiplicity surveys of the last decade and a half have shown a surprising diversity of visual binary frequency in nearby star forming regions (Ghez et al. 1993; Leinert et al. 1993; Simon et al. 1995; Patience et al. 2002). Taurus is particularly rich in multiples, however, other regions appear to have solar neighborhood stellar companion frequency (Petr et al. 1998; Beck et al. 2003; Ratzka et al. 2005). The differences appear to result from the influence of initial conditions in these regions on the frequency of binary formation (Mathieu et al. 2000; Sterzik et al. 2003; Köhler et al. 2006). The frequency of spectroscopic binaries in the same regions which have been so well-studied for visual binaries is not as well-known. The early, 1 to a few km s^{-1} precision radial velocity measurements of Herbig (1977), Hartmann et al. (1986), Walter et al. (1988; 1994), Mathieu et al. (1989), and Mathieu (1994) identified the largest samples of spectroscopic binaries in the Taurus and Ophiuchus star forming regions published to date. Recent radial velocity surveys of young stars (e.g., Guenther et al. 2001; Melo 2003; Huerta et al. 2005; Covey et al. 2006; Joergens 2006; Kurosawa et al. 2006) for stellar and substellar companions are just beginning to produce results. Some of these next generation surveys are larger in scope and some are higher in precision than previous work. Large, complete surveys drawn from consistent samples are not yet available but will provide extremely useful input for theorists studying binary and planet formation (e.g., Delgado-Donate et al. 2004; Boss 2006).

Besides extending our knowledge of young star multiplicity to very low masses, spectroscopic binaries are important in their own right. Such systems allow precise determination of dynamical properties such as the mass function (for single-lined systems, SB1s), the mass ratio (for double-lined systems, SB2s), and ultimately component masses (for SB2s which are eclipsing or have angularly resolved orbits, yielding orbital inclination). Mass is the single most important stellar property from which, given the metallicity, all other properties of an object may be derived. Accurate masses are necessary to calibrate the theoretical pre-main-sequence (PMS) evolutionary tracks (Simon et al. 2000; Hillenbrand & White

2004), particularly at low masses where there is significant scatter in models and very few objects with known masses (White et al. 1999; Prato et al. 2002a; Torres & Ribas 2002; Stassun et al. 2006). Furthermore, mass ratio distributions and secondary mass distributions provide additional input to theories of binary formation. Thus, the identification of young spectroscopic binaries is extremely useful. Young M stars are of particular interest in that they are the most common stellar spectral type in most star forming regions, including Ophiuchus, regardless of where exactly the mass function turns over near the substellar boundary (e.g., Luhman et al. 2000).

There are very few young, low-mass SB2s known. Only 12.9% of the 31 SB2s listed in Prato et al. (2002a) have primary masses less than 1 solar mass. Although additional PMS SB2s have been discovered since 2002, the small percentage of sub-solar mass systems prevails. The reason for this bias is natural: surveying low-mass stars in SFRs with minimum distances of ~ 140 pc, and therefore relatively faint magnitudes, is impractical at 1–3 m class telescopes where most of the radial velocity studies of young stars have been conducted with visible light spectrometers. Furthermore, radial velocity surveys for long-period systems, or for systems with very low-mass companions, require long time series observations. The 8–10 m class telescopes have only been fully equipped and commissioned in the last 5–10 years, therefore work of this nature has only recently become possible.

My colleagues and I have developed a powerful approach to the study of SBs using high-resolution infrared spectroscopy (Prato 1998; Steffen et al. 2001; Prato et al. 2002a, b; Mazeh et al. 2002; 2003; Simon & Prato 2004). Low-mass primary stars emit most of their radiant energy at wavelengths $>1 \mu\text{m}$. Also, because luminosity scales as a steeper function of mass in the V -band than, for example, in the H -band, it is easier to detect faint, low-mass secondary stars in the blended spectra of SBs at longer wavelengths. Finally, the lower amplitude of star spot modulated fluctuations in the infrared compared to visible light also favors longer wavelength observations (Carpenter et al. 2001). It is simply most efficient to search for young M star spectroscopic binaries with a large aperture telescope in the infrared.

This paper describes the initial results from a radial velocity survey of a homogeneous sample of M stars in the Ophiuchus SFR with infrared observations at the Keck II 10-m telescope. The goal was to find young M star spectroscopic binaries in Ophiuchus by searching for radial velocity variability and to measure the mass ratios of any new systems discovered. Two SB2s, two SB1s, and one radial velocity variable were found. The results presented are preliminary in this first report; because the phase coverage is sparse, it is only possible at this point to measure mass ratios. Determination of the periods and other orbital elements will require intensive followup. A natural outcome of observing with a

large aperture telescope located at a site with good seeing was the additional, serendipitous discovery of a number of close, visual binaries. In §2 I describe the sample selection and the template star library used for radial velocity measurements. The observations and data reduction are detailed in §3. The results are presented in §4. §5 provides a discussion and a summary appears in §6.

2. Sample Selection and Spectral Type Templates

All the targets were culled from the spectroscopic classification paper of Martín et al. (1998). The objects in that paper were selected for association with *ROSAT* X-ray sources, i.e. location within $30''$, and optical brightness, i.e. $V \leq 15$ mag. The *2MASS* *H*-band magnitudes of my sample range from 8.6 to 11.1 and the spectral types, as presented in Martín et al., from K6 to M4.5 (but see §4.1). This is not a complete sample; seven K6 and K7 stars and five M stars from Martín et al. were not observed. However, it is a homogeneous sample in that all of the targets are X-ray sources, are located in Ophiuchus, and are young. Martín et al. determined youth and membership with Li 6708Å measurements.

I originally chose 31 M star targets in 28 fields; several fields around the coordinates given in Martín et al. (1998) contained multiple candidates. In one such field (RX J1625.2–2455), two spectra taken of the fainter object, “b” in Table 1 of Martín et al., revealed a large radial velocity (~ 130 km s $^{-1}$). This object was subsequently excluded from the sample as a probable halo star. It is likely the brighter “a” component that is associated with the large Li equivalent width in Table 2 of Martín et al.. Both components in three of the subarcsecond, visual binaries, discovered in this study, were observed individually. Thus the final number of unresolved objects surveyed in this paper is 33, located in 30 distinct systems. Four of these are classical T Tauri stars (CTTS), 24 are weak-lined T Tauri stars (WTTS), and 5 are post-T Tauri stars (PTTS), according to the classification of Martín et al. Among the distinct regions within Ophiuchus described in Martín et al., I selected 2 targets from the “streamers”, 12 from the “ ρ Oph core”, 7 from “R7”, and 12 from the “smoke rings” (see Martín et al. Figure 1). The target names appear in Table 1, column (1). Accurate coordinates for the objects were determined by iterating and refining the initial coordinates using the *2MASS* interactive image service; these appear in columns (2) and (3) of Table 1. If two relatively bright stars appeared in the same field near the coordinates given by Martín et al. and were both observed, they are designated with the same name followed by a letter indicating cardinal orientation. The PMS evolutionary class, CTTS (C), WTTS (W), or PTTS(P), from Martín et al. is given in column (4) of Table 1.

A subset of the spectral type templates from Prato et al. (2002a) and Bender et al.

(2005) were used in this current study to measure radial velocities. Figure 1 of Prato et al. shows the spectral types of these templates as given in SIMBAD. The FeI and OH features at $\sim 1.563\mu\text{m}$ are especially useful in the determination of spectral types. In order to assign spectral types to the targets and to thereby determine which templates to use for radial velocity measurements, I reordered the sequence of M0 to M4 templates to show a logical progression of FeI and OH features. T. Barman kindly produced a synthetic sequence of Phoenix model spectra from the NexGen grid (Hauschildt et al. 1999) over a similar temperature range for comparison. I assigned spectral types to the M type template stars on the basis of their atomic and molecular features and used the synthetic sequence as a guide (Figure 1 and Table 2). Interestingly, with the exception of the first (M0) and last (M4) objects in this series, the best progression that I identified differs from the spectral types for these standards adopted in the literature, based primarily on low- to medium-resolution visible light spectroscopy. Prato et al. (2002b) also note this mismatch. This discrepancy is likely the result of a number of factors. The visible and infrared light spectra do not necessarily sample the same regions in the M star atmospheres. Furthermore, at the high-resolution ($\sim 30,000$) of the infrared observations, the spectra are likely affected by subtle differences in atmospheric mixing, metallicity, surface gravity, etc. (J. D. Kirkpatrick, priv. comm.).

3. Observations and Data Reduction

All data were obtained at the Keck II 10-m telescope on Mauna Kea using NIRSPEC, the facility near-infrared, cross-dispersed, cryogenic spectrometer (McLean et al. 1998; 2000). NIRSPEC employs a 1024×1024 ALADDIN InSb array detector. I observed in the H -band, at a central wavelength of $\sim 1.555\mu\text{m}$, with an $0.288''$ (2 pixel) $\times 24''$ slit, yielding $R=30,000$. Dispersion solutions were derived from OH night sky emission lines for all spectra; these are very well distributed across order 49, the central order at this setting. Another advantage of order 49 is the relative lack of telluric absorption lines in the region. Consequently, I did not divide out telluric standard spectra and used only order 49 in the subsequent analysis. Source acquisition was accomplished with the slit viewing camera, SCAM, which utilizes a 256×256 HgCdTe detector with $0.18''$ pixels.

The observations were made between March, 2002, and July, 2004. H -band magnitudes for the sample range from 8.6 to 11.1; total integration times depended on source brightness and seeing and typically varied from 10–40 minutes, in individual frames of 100–300 s. Three to four spectra were taken for almost all of the targets over the 3 years of observations. For one star, only one spectrum was obtained; for another, only two spectra were obtained. The

2MASS H -band magnitudes for the targets and the number of NIRSPEC observations are listed in columns (5) and (6) of Table 1.

The REDSPEC package, software designed at UCLA by S. Kim, L. Prato, and I. McLean specifically for the analysis of NIRSPEC data¹, was used for all reductions. The observational set up and data reduction procedures followed were identical to those described in Prato et al. (2002a). This is true for both target stars as well as the spectral type template stars used in the analysis here. Although most of the template stars were observed on runs in 2000–2001 during which NIRSPEC was used in conjunction with the Keck II adaptive optics (AO) system (Prato et al.; Mazeh et al. 2003), this does not introduce any significant differences in the resultant spectra. The same is true for the one target spectrum taken with NIRSPEC behind the AO system.

For the three visual binaries (§4.2) discovered during the course of these observations which had the angularly resolvable separations of $0.7''$ to $1.0''$ in conditions of good seeing (0.4 – $0.8''$), both objects were usually placed on the appropriately rotated slit and observed simultaneously. For RX J1612.6–1924E, only once were both components observed in this way. The traces of the wider pairs were easily separable. For the closest visual pair, narrow apertures were used to sum the flux from each component, on the outside extremes of the spectral traces in order to avoid contamination of each spectrum by the other. A cross-cut of the trace of an apparently single target was used to judge the extent of the overlapping zone to avoid.

4. Results

4.1. Spectral Types, Radial Velocities, and Spectroscopic Binaries

The spectral types for the sample, estimated from comparison with the template stars shown in Figure 1, are given in column (7) of Table 1 and range from K7 to M4. Some spectral types listed in Table 1 differ from those found by Martín et al. (1998) (using moderate resolution, visible light spectroscopy) by up to 2 spectral classes. However, most typically agree to within 1 spectral class with Martín et al.’s results. Radial velocities were measured for the targets by cross-correlating each spectrum of a particular target against the closest matching template, rotationally broadened to the best fit $v \sin i$. Rotational broadening of the template spectra was accomplished using routines developed by C. Bender (priv. comm.), following Gray (1992) with the limb-darkening law of Claret (2000). Both spectral type and

¹See: <http://www2.keck.hawaii.edu/inst/nirspec/redspec/index.html>

estimated $v \sin i$ were determined by visual inspection of the spectra and assumed to apply to all the data for an individual object. The cross-correlation peaks were fit with Gaussian functions to determine the radial velocities.

The uncertainty in velocity measurements depends in part on how well it is possible to measure the radial velocities of the template standard stars with NIRSPEC. For the template library used here, the systematic uncertainty was estimated at $\sim 1 \text{ km s}^{-1}$ (Prato et al. 2002a; Mazeh et al. 2003). Column (8) of Table 1 shows the average radial velocities measured for each young star target in this sample and column (9) provides the rms scatter for each object, $\sigma_{v_{rad}}$. The average $\sigma_{v_{rad}}$ for the 30 objects in Table 1 with more than one velocity measurement, excluding the two obvious SB2s, is 0.90 km s^{-1} . All objects with $\sigma_{v_{rad}}$ greater than about five times this average are defined as SBs. I categorize one object with $\sigma_{v_{rad}} = 3.22 \text{ km s}^{-1}$ as radial velocity variable. If the two SB1s, the radial velocity variable, and ROXR1 31, for which the observed signal to noise ratio was rather low for one epoch (see §4.3.6), are also removed from the calculation, the average $\sigma_{v_{rad}}$ is 0.43 km s^{-1} . I therefore define the *internal* uncertainty in the radial velocity variability measurements as 0.43 km s^{-1} .

In Table 1, each of the 33 targets observed individually for spectroscopic multiplicity is listed separately. There are two SB2s, 2 SB1s, and one radial velocity variable. The primary star velocities for the SB1s and the radial velocity variable appear in Table 3. For the SBs, both the primary and secondary star velocities, along with the mass ratios and center of mass velocities, are given in Table 3 (see also §4.3). The spectral types for the SB2s were derived from the spectra taken during minimum radial velocity difference between the components. This was the orbital configuration when the first spectrum was taken for both SB2s; thus, both initially appeared single. Because the mass ratios are both close to unity, the spectral types are unlikely to differ by more than one spectral class. Assuming that all of the newly discovered SB pairs presented here have equal flux ratios, if angularly resolved, none of the primary stars' magnitudes would fall below $H = 11.1$, the magnitude of the faintest object in the survey. Thus, there is no bias towards inclusion of binaries in the sample based on brightness.

4.2. Visual Binaries

The excellent seeing often afforded on Mauna Kea revealed that a number of the systems studied here have close visual companions, identified by inspection of the SCAM images. Greene & Young's (1992) study of infrared sources in the ρ Oph core region showed that the surface density of background *field stars*, appearing in the same region as the young

stars with K magnitudes of <13 , is 0.07 per square arcminute, or 1.9×10^{-5} field stars per square arcsecond. For M stars, the $H - K$ colors are at most ~ 0.3 mag, so K -band data are an adequate surrogate for H -band observations. Assuming a similar contamination surface density in all of the Ophiuchus sub-regions I surveyed, there is a 72% chance of one interloper within $20''$ of the 30 systems observed and an 18% chance of an interloper within $10''$. The probability of a subarcsecond interloper is $<1\%$ for the 30 systems on the whole.

The contamination from the denser distribution of *young* stars in the ρ Oph core is 3.4 times greater than from field stars. Thus the chance for a superposition of a young star within $10''$ of one of the target stars is 63%. I therefore adopt a $10''$ upper limit for a probable physical binary companion, consistent with that used by Simon et al. (1995). Given that the R7, streamers, and smoke ring regions are probably less dense than the ρ Oph core region, this is likely an upper limit on the young star contamination probability.

In total, I discovered five visual binary systems with separations of $\sim 1''$ or less, all located in the smoke rings and R7. For three of these pairs it was possible to take individual spectra of both components (§3), hence the 33 individual, unresolved objects surveyed for radial velocity variability. The separations of the other two subarcsecond binaries were too small to obtain spectra of each component without NIRSPEC behind the AO system (Comments, Table 1).

There are two targets with companions between $1''$ and $10''$; in one case a fainter, presumably later type star is $\sim 7''$ away from RX J1613.8–1835, and in the other, an F star is located just under $10''$ from RX 1621.4–2332 (Vrba et al. 1993). Four more systems have companions between $10''$ and $20''$. Two of these are listed as distinct targets. The other two were observed once but do not appear to be young M stars; one is ScoPMS 52, a K0 star (Walter et al. 1994) and the other, $\sim 17''$ west of RX J1612.6–1924, has a featureless spectrum. One of the SB2s comprises one component of a subarcsecond pair (RX J1622.7–2325Nw); the other component in this $0.9''$ pair is an $0.1''$ binary (RX J1622.7–2325Ne), revealed serendipitously with AO. The $1''$ separation pair RX J1612.6–1924Ew–Ee harbors at least one radial velocity variable. To search for visual companions with separations smaller than $\sim 0.4''$ it will be necessary to carefully observe this sample with AO; initial AO snap-shot observations of about half the sample will be discussed in a future paper.

4.3. Comments on Individual Systems

4.3.1. *RX J1612.3–1909*

The four spectra of this SB1 system reveal rapid rotation on the order of $v \sin i \sim 40\text{--}50 \text{ km s}^{-1}$. As a result, the determination of spectral type is challenging. A broad, boxy feature at $\sim 1.563 \mu\text{m}$ suggests that it is earlier than the M2.5 designation of Walter et al. (1994) and Martín et al. (1998). Figure 1 shows this spectral region for the template standard stars. An M2.5 spectrum, rotationally broadened to 50 km s^{-1} , would show a fairly triangular feature at $\sim 1.563 \mu\text{m}$. I have therefore classified it as an M1. A recent low-dispersion, visible light spectrum is consistent with this classification (F. Walter, priv. comm.).

In addition to making the spectral type classification more difficult, broad absorption lines can complicate cross-correlation and yield less precise measurements of radial velocity. The four radial velocities measured for RX J1628.0–2448 appear in Table 3. In order to investigate the possibility that their variability is the result of poor measurement precision resulting from broad spectral lines, I examined the cross-correlation results for the other $v \sin i \sim 50 \text{ km s}^{-1}$ target in the sample, RX J1628.0–2448. Cross-correlation of an M2 template spectrum, rotated to 50 km s^{-1} , against RX J1628.0–2448 produced the identical radial velocity for the spectra from two epochs taken ~ 1 year apart. This lends confidence to the SB1 designation of RX J1612.3–1909; over the 14 months during which the 4 spectra were taken the velocity varied by as much as 14 km s^{-1} .

4.3.2. *RX J1612.6–1924E*

About $17''$ away to the west of RX J1612.6–1924E is an object with a featureless spectrum; however, the coordinates listed under RX J1612.6–1924 in SIMBAD point to that object. Hence the eastern target is specified as “E” in Table 1 to avoid confusion. RX J1612.6–1924E is itself a $1''$ binary. Both components of this visual pair were observed, although, unfortunately, RX J1612.6–1924Ee only once. Assuming an uncertainty of 1 km s^{-1} for this single radial velocity measurement, $\sim -12 \text{ km s}^{-1}$, indicates that it is off from the sample average of -6.8 km s^{-1} , excluding only the four SBs, by 5σ . RX J1612.6–1924Ew was observed 3 times and shows a radial velocity rms in these measurements of 3.22 km s^{-1} . I therefore characterize Ew as a radial velocity variable. The radial velocities of the two RX J1612.6–1924E components should be measured again to determine if one or both of these stars are SBs.

4.3.3. *RX J1622.7–2325N*

An M0.5 star also lies $\sim 13''$ to the south of this system, designated as RX J1622.7–2325S in Table 1. RX J1622.7–2325N is an $0.9''$ binary. The eastern component is an $0.1''$ pair discovered serendipitously in an AO observation in February, 2005, with the NIRC2 camera on Keck II. RX J1622.7–2325Nw is an SB2 with a mass ratio of $q=0.94\pm0.03$ and a center of mass velocity $\gamma = -6.21\pm0.82 \text{ km s}^{-1}$, consistent with the non-SB sample average. Figure 2 shows the spectra from the 4 epochs of observation. The primary versus secondary radial velocities, easily determined from the double peaks in the cross-correlation plots, are plotted in Figure 3 and tabulated in Table 3. For the three epochs during which the two stars in the SB showed distinct radial velocities, the correlation peak of the primary was always slightly larger than that of the secondary. The mass ratio is the negative of the slope of the fit to these points and the γ velocity is equal to the y-intercept divided by $1+q$ (Wilson 1941). The uncertainties in the slope and y-intercept were determined by a linear fit to the velocity data taking into account the errors in both v_1 and v_2 (Table 3). These uncertainties were then propagated to determine the uncertainty in q and γ .

To determine an upper limit for the period of the system I assumed component masses of $0.65 M_{\odot}$ for each star in the SB2 (Luhman 2000). The maximum velocity amplitude measured for the primary star was $\sim 51 \text{ km s}^{-1}$. Therefore, given $q=0.94$, the period must be less than 11 days. A less stringent estimate may also be made on the basis of the spectra themselves. The component radial velocities (Table 3) for the second and third epochs of observation of RX J1622.7–2325Nw were almost identical, implying that the system had completed at least one full orbit between those observations, taken 33 days apart.

4.3.4. *RX J1622.8–2333*

Because the $v \sin i$ of this SB1 is about 25 km s^{-1} it should be possible to analyze the spectra to identify the secondary component and convert it into an SB2 (e.g., Prato et al. 2002a). However, with no a priori knowledge of the orbital elements, this will require more than the 4 observations acquired as part of this work. Application of a two-dimensional cross-correlation algorithm, such as TODCOR (Zucker & Mazeh 1994) may also help to identify the secondary. It is possible that either the mass ratio is small or the inclination of the system is close to face on: no evidence for lines of the secondary star were found in the one-dimensional cross-correlation analysis used. The maximum observed velocity variation was on the order of 9 km s^{-1} (Table 3). The second and third epoch velocities are similar, again providing an upper limit for the period of the system, in this case 80 days.

4.3.5. ROXR1 14

ROXR1 14 is an SB2 with $q=0.98\pm0.02$ and $\gamma = -6.16\pm0.43 \text{ km s}^{-1}$, consistent with the non-SB sample average radial velocity. Figure 4 shows the spectra from the 4 epochs of observation. The primary versus secondary velocities, determined as for RX J1622.7–2325Nw, are shown in Figure 5, and tabulated in Table 3. The best linear fit to the data, including the velocity errors, was used in the determination of q and γ and their associated uncertainties. As for RX J1622.7–2325Nw, the correlation peak of the primary was always slightly larger than that of the secondary when separable.

Making the same assumptions regarding systemic mass as for RX J1622.7–2325Nw, i.e. $M_{tot} = 1.3M_{\odot}$, combined with a maximum measured primary radial velocity amplitude of 40 km s^{-1} and $q=0.98$, yields an upper limit for the period of ROXR1 14 of 24 days. There were no measurements of identical velocities made close in time to provide additional information.

4.3.6. ROXR1 31

Despite the anomalous rms scatter in the 3 radial velocity measurements of this system, it is unlikely that ROXR1 31 is a radial velocity variable. Two of the measurements, of spectra with similarly high signal to noise (~ 200), were very close, -7.01 km s^{-1} and -7.84 km s^{-1} . For the other observation, made during deteriorating weather conditions, the signal to noise is only ~ 60 and the radial velocity measured is -4.13 km s^{-1} . Although a follow-up measurement of this target will be important to conclusively rule out radial velocity variability, this is likely an example of the loss of precision associated with poor signal to noise observations.

4.4. Cluster Velocities

Excluding the four SBs, the radial velocity variable, and the object observed only on one occasion (RX J1612.6-1924Ee), the average radial velocity of the sample is $-6.27 \pm 1.48 \text{ km s}^{-1}$. This agrees well with the average radial velocity, $-6.3 \pm 1.0 \text{ km s}^{-1}$, found for several ρ Oph objects and about a dozen nearby Upper Scorpius very low-mass young targets (Kurosawa et al. 2006). The average radial velocities of the three sub-regions studied here, in which more than 2 stars were observed, are also statistically indistinguishable from the overall average. This implies, as underscored in Kurosawa et al., that a single velocity measurement that is more than $2\text{--}3 \sigma$ from this mean should be repeated to search for potential radial velocity

variables. Indeed, RX J1612.6-1924Ee may turn out to be a spectroscopic binary and, on the basis of its discrepant radial velocity, certainly merits follow-up observations (§4.3.2). However, both of the SB2s discovered here were initially observed, coincidentally, at phases during which the stellar motions were tangential to the line of sight. At least two radial velocity measurements may therefore be crucial. Covey et al. (2006) measured the radial velocities of a sample of Class I protostars and compared these to the velocity of the local CO gas. They identify one candidate radial velocity variable M star in Ophiuchus using this approach.

The constancy of the velocity dispersion in the areas around the ρ Oph core, as well as in the more distant smoke rings region and in Upper Scorpius, provide input as to the nature of star formation in this molecular cloud complex. Feigelson (1996) argues that this implies a slow and continuous rate of star formation over a long period, after which thermal motions disperse the members with a spread of ~ 1 km s $^{-1}$. The Chamaeleon cloud presents a similar star formation history, in contrast to that observed in the discreet bursts of star formation in isolated cloudlets, as observed in the Taurus-Auriga complex (Feigelson).

5. Discussion

5.1. Spectroscopic Multiplicity and Comparison to Literature

The spectroscopic multiplicity of the low-mass targets listed in Table 1 is 4/33, or $12.1\%_{-3.6\%}^{+7.9\%}$. The uncertainties were determined using a binomial probability distribution, after Burgasser et al. (2003). Including the radial velocity variable, RX J1612.6–1924Ew (§4.3), the spectroscopic multiplicity is 5/33, or $15.2\%_{-4.3\%}^{+8.1\%}$. Mathieu et al. (1989) found a similar SB fraction in their study of weak-lined T Tauri stars in the Taurus-Auriga, Scorpius-Ophiuchus, and Corona Australis star-forming regions, $9\% \pm 4\%$, although their sample consists of primarily G and K spectral type systems. Indeed, only 2 out of the 25 young SBs listed in Mathieu (1994) are M stars. The short period SB frequency of field stars is indistinguishable, $12\% \pm 3\%$ (Abt & Levy 1976; Morbey & Griffin 1987; Abt 1987). These samples described in the literature, however, are not as narrowly defined as the sample in the present survey. The range of spectral types, as determined herein, cover a relatively flat distribution from K7 to M4 with a median value of M1, corresponding to a mass range of about 0.3–0.7 M_{\odot} for ages of a few Myr (Baraffe et al. 1998; Luhman 2000). Almost half of this sample are M0 to M1 stars.

Early surveys of T Tauri stars for SBs described by Mathieu et al. (1989) and Mathieu (1994) considered higher mass objects, such as the sample of Walter et al. (1988; Table 1), on

average about two times more massive than the sample described here. Thus, although recent results from the surveys of Joergens (2006) and Kurosawa et al. (2006) have focussed mainly on samples of about a dozen young substellar objects (i.e. targets of spectral type later than M6) and a few very low mass (spectral type M2.5–M5.5) stars, this paper describes the largest homogeneous survey of low-mass T Tauri stars to date. The average spectral type of those presented in Table 1 is M1. Three of the four SBs are systems with M1 star primaries; the fourth has a K7 primary. Although the occurrence of SBs is greater therefore in the higher mass bins, it is consistent with the distribution of masses studied. It is unlikely that any SBs were missed in the lower mass bins on the basis of poor radial velocity precision as the scatter in radial velocity measurements is indistinguishable between the early and late spectral type bins.

Melo (2003) draws attention to an excess in the frequency of spectroscopic binaries in Ophiuchus compared to other small SFRs, such as Taurus. SBs were identified in the three sub-regions with more than two stars surveyed, the smoke rings, R7, and L1688 core. Surveys parallel to this one, including similar sample sizes selected with the same criteria, will help to verify a true differences between molecular cloud complexes. Currently, the numbers of young stars in any given region observed for spectroscopic multiplicity are small and the samples irregular. For example, observations by Melo (2003) of about a dozen systems in Scorpius-Ophiuchus, 8 of them visual binaries, did not angularly resolve the components. In some cases, double lines can be detected if one or both components of a visual binary are SBs; however, the blended light from three or more stars can also disguise the signal from a low-mass or long-period companion.

Reipurth et al. (2002) studied a sample of ~ 100 young stars in mainly southern SFRs and identified 2 SBs and 5 radial velocity variables. Those authors conclude that a contributing factor to the low spectroscopic multiplicity detected may be attributable to complications arising from observations of the complex, classical T Tauri star spectra. My sample contains 4 classical systems, none of which were found to be spectroscopic binaries or even radial velocity variables. However, the average rms radial velocity scatter of these 4 targets, $\sim 0.6 \text{ km s}^{-1}$, is fairly consistent with that of the non-SB average: $\sim 0.43 \text{ km s}^{-1}$. Therefore, it is possible that the low SB detection rate of Reipurth et al. resulted from other factors as well, such as the relatively blue wavelength range of their observations, 3600–5200 Å, subject to stronger veiling from accretion processes in classical T Tauri stars than *H*-band observations. The slightly lower resolution of their spectra, 20,000, might also account for the lower detection rate. It is also possible that Ophiuchus is unusually rich in spectroscopic binaries as noted above, and that few of the Reipurth et al. targets besides Haro 1-14c were located in this region.

5.2. Potential Limitations of Survey

In order to estimate the sensitivity of this survey to small mass ratio systems, I consider a test case in which a 5 km s^{-1} primary star amplitude was measured in a 3 year period, i.e. the duration of this survey. This amplitude is consistent with the largest velocity change measured for radial velocity variable RX J1612.6–1924Ew. Assuming that one fourth of the orbit is traversed in 3 years, the total orbital period is 12 years². For an SB with an edge-on, circular orbit, and given $v_1 = 5 \text{ km s}^{-1}$ and $P=12$ years, the present study is sensitive to early M star SBs with mass ratios, $q=M_2/M_1$, down to 0.6 (Figure 6). Observations of shorter period systems, however, are sensitive to smaller values of q . For a primary star mass of $\sim 0.6 M_\odot$ and a mass ratio of 0.1, the velocity modulation of the primary in an edge-on circular orbit will only be detectable at 5 km s^{-1} for periods of $\lesssim 40$ days, or 0.11 years. This illustrates the strong bias towards detection of unity mass ratio systems among longer period SBs. Mass ratio distributions of SBs over a wide range of periods will reflect this bias; however, improved velocity precision will help to alleviate this limitation. The 5 km s^{-1} radial velocity amplitude is also conservative; a 5σ detection and the internal radial velocity uncertainty of 0.43 km s^{-1} implies that measuring a 2.5 km s^{-1} should be achievable using the simple techniques applied here. With a 2.5 km s^{-1} primary velocity amplitude, a system with a mass ratio of 0.1 and an $\sim 0.6 M_\odot$ primary could be detected with a period as long as about 310 days.

The star spots which are common and at times abundant on young, active stars can affect radial velocity measurements (Saar & Donahue 1997). One of the most active weak-lined T Tauri stars known, Parenago 1724, manifests a star spot induced periodic radial velocity modulation of $\sim 5 \text{ km s}^{-1}$ (Neuhauser et al. 1998). The SB1s and SB2s identified in this sample have primary star velocity variations of 9–80 km s^{-1} . Thus spot induced apparent radial velocity modulation is probably not significant.

6. Summary

I have surveyed a homogeneous sample of young ($\sim 1 \text{ Myr}$) M stars in the Ophiuchus SFR. The goals of this program were to identify the SB frequency of the sample, measure mass ratios of SB2 pairs, and begin to search for long-period systems suitable for high-

²A binary comprised of two young M1 stars, with total mass $1.3 M_\odot$ (Luhman 2000), and $P=12$ years would have an angular separation of $\sim 0.04''$ at a distance of 140 pc. This separation is equivalent to the diffraction limit of the Keck II telescope in the H -band and therefore provides a convenient definition for a spectroscopic versus a visual binary.

angular resolution and interferometric orbit mapping. The following points summarize the conclusions of this work:

- (1) Including all of the spectroscopic and visual binary components detected, I detected evidence for a total of 41 stars in this sample, located in 30 systems. 33 individual targets were observed spectroscopically to search for variable radial velocities.
- (2) There are 2 SB2s, 2 SB1s, and at least 1 radial velocity variable. An internal precision of 0.43 km s^{-1} was achieved.
- (3) The average spectral type of the sample was M1; three of the SB primaries are M1 stars and one is a K7. The objects in the sample are located in 4 sub-regions of Ophiuchus. The average radial velocity of the entire sample and of the individual sub-region objects is indistinguishable, supporting a scenario for continuous star formation across this molecular cloud complex.
- (4) Counting the 4 identified SBs in 33 systems, the spectroscopic binary frequency in this sample is $12\%_{-3.5\%}^{+8.0\%}$, similar to that found by previous spectroscopic studies of higher mass young stars as well as field stars. Therefore, there appears to be no dearth of low-mass, stellar SBs in Ophiuchus.
- (5) The sample is rich in visual binary pairs; this work revealed 3 new visual binaries, all of separation $\leq 1''$. A hierarchical quadruple was also identified: RX J1622.7–2325N is an $0.9''$ pair within which the eastern star is an $0.1''$ binary and the western one an SB2.
- (6) Both the SB and visual binary frequencies measured here are almost certainly incomplete. Adaptive optics or *HST* observations will reveal additional angularly resolved components. Followup observations to identify long-period, highly eccentric, and low-mass ratio SBs will also be important for a more stringent completeness limit. The coincidence that the SB2s discovered in this modest survey were both initially observed when their components were close to the gamma velocity of the system underscores the importance of multiple observations and broad phase coverage. Inspection of the first epoch spectra alone did not reveal obvious double-lined structure. At least one additional epoch of identical spectroscopic observations of this sample may reveal additional SBs and confirm the radial velocity variable. High angular resolution imaging may detect more visual binaries. Denser sampling is required to determine the orbital elements of the new SBs discovered. Properties of this rich, initially X-ray identified sample, such as extinction, circumstellar dust, rotational velocities, and a more complete discussion of visual binarity will be presented in a future paper.

These observations benefitted from the expert operating skills of the Keck OAs, in particular C. Wilburn, G. Puniwai, C. Sorenson, J. Aycock, S. Magee, and T. Stickel. Excellent support, technical and logistical, was provided by G. Hill, J. Lyke, P. Opoki, P. Amico, and B. Schaefer. I am grateful to M. Simon for a thorough reading of a draft of this paper, to

O. Franz for a final vetting, and to T. Barman, D. Kirkpatrick, H. Roe, M. Simon, B. Skiff, and F. Walter for advice and information. I acknowledge helpful encouragement early on in this project from E. Becklin, M. Rich., and I. McLean. The latter in particular provided both the financial support for the initial stages of this work as well as the academic freedom that allowed me to develop it. I thank the anonymous referee for thoughtful comments that helped to improve the presentation of this paper. NSF grant AST 04-44017 and awards from the Keck PI Data Analysis Fund to L. Prato have financed the majority of this research. I am grateful to the NASA Keck TAC for the adequate time allocations to conduct and complete this multi-semester program. This work made use of the SIMBAD reference database, the NASA Astrophysics Data System, and the data products from the Two Micron All Sky Survey, which is a joint project of the University of Massachusetts and the Infrared Processing and Analysis Center/California Institute of Technology, funded by the National Aeronautics and Space Administration and the National Science Foundation. Data presented herein were obtained at the W.M. Keck Observatory from telescope time allocated to the National Aeronautics and Space Administration through the agency’s scientific partnership with the California Institute of Technology and the University of California. The Observatory was made possible by the generous financial support of the W.M. Keck Foundation. I recognize and acknowledge the significant cultural role that the summit of Mauna Kea plays within the indigenous Hawaiian community. I am very grateful for the opportunity to conduct observations from this special mountain.

REFERENCES

- Abt, H. A., & Levy, S. G. 1976, *ApJS*, 30, 273
- Abt, H. A. 1983, *ARA&A*, 21, 343
- Abt, H. A. 1987, *ApJ*, 317, 353
- Baraffe, I., Chabrier, G., Allard, F., & Hauschildt, P. H. 1998, *A&A*, 337, 403
- Beck, T. L., Simon, M., & Close, L. M. 2003, *ApJ*, 583, 358
- Bender, C., Simon, M., Prato, L., Mazeh, T., & Zucker, S. 2005, *AJ*, 129, 402
- Boss, A. P. 2006, *ApJ*, 643, 501
- Burgasser, A. J., Kirkpatrick, J. D., Reid, I. N., Brown, M. E., Miskey, C. L., & Gizis, J. E. 2003, *ApJ*, 586, 512
- Carpenter, J. M., Hillenbrand, L. A., & Skrutskie, M. F. 2001, *AJ*, 121, 3160

- Claret, A. 2000, A&A, 363, 1081
- Covey, K. R., Greene, T. P., Doppmann, G. W., & Lada, C. J. 2006, AJ, 131, 512
- Delgado-Donate, E. J., Clarke, C. J., Bate, M. R., & Hodgkin, S. T. 2004, MNRAS, 351, 617
- Duquennoy, A., & Mayor, M. 1991, A&A, 248, 485
- Feigelson, E. D. 1996, ApJ, 468, 306
- Ghez, A. M., Neugebauer, G., & Matthews, K. 1993, AJ, 106, 2005
- Gray, D. F. 1992, *The Observation and Analysis of Stellar Photospheres* (New York: Wiley)
- Greene, T. P., & Young, E. T. 1992, ApJ, 395, 516
- Guenther, E. W., et al. 2001, in Zinnecker H., Mathieu R. D., eds, Proc. IAU Symp. 200, *The Formation of Binary Stars*. Astron. Soc. Pac., San Francisco, p. 165
- Hartmann, L., Hewett, R., Stahler, S., Mathieu, R. D. 1986, ApJ, 309, 275
- Hauschildt, P. H., Allard, F., Baron, E. 1999, ApJ, 512, 377
- Herbig, G. H. 1977, ApJ, 214, 747
- Hillenbrand, L. A., & White, R. J. 2004, ApJ, 604, 741
- Huerta, M., Prato, L., Hartigan, P., Johns-Krull, C. M., & Jaffe, D. T. 2005, BAAS, 207, 6809
- Joergens, V. 2006, A&A, 446, 1165
- Köhler, R., Petr-Gotzens, M. G., McCaughrean, M. J., Bouvier, J., Duchêne, G., Quirrenbach, A., & Zinnecker, H. 2006, astro-ph/0607670
- Kurosawa, R., Harries, T. J., & Littlefair, S. P. 2006, MNRAS, 372, 1879
- Leinert, Ch., Zinnecker, H., Weitzel, N., Christou, J., Ridgway, S. T., Jameson, R., Haas, M., & Lenzen, R. 1993, A&A, 278, 129
- Luhman, K. L. 2000, ApJ, 544, 1044
- Luhman, K. L., et al. 2000, ApJ, 540, 1016
- Marcy, G. W., & Butler, R. P. 2000, PASP, 112, 137

- Martin, E. L., Montmerle, T., Gregorio-Hetem, J., & Casanova, S. 1998, MNRAS, 300, 733
- Mathieu, R.D., Walter, F.M., & Myers, P.C. 1989, AJ, 98, 987
- Mathieu, R. D. 1994, ARA&A, 32, 465
- Mathieu, R. D., Ghez, A. M., Jensen, E. L. N., & Simon, M. 2000, in Protostars and Planets IV, ed. V. Mannings, A. P. Boss, & S. S. Russell (Tucson: Univ Arizona Press), 703
- Mazeh, T., Goldberg, D., Duquennoy, A., & Mayor, M. 1992, ApJ, 401, 265
- Mazeh, T., Prato, L., Simon, M., Goldberg, E., Norman, D., & Zucker, S. 2002, ApJ, 564, 1007
- Mazeh, T., Simon, M., Prato, L., Markus, B., & Zucker, S. 2003, ApJ, 599, 1344
- McLean, I. S., et al. 1998, SPIE, 3354, 566
- McLean, I. S., Graham, J. R., Becklin, E. E., Figer, D. F., Larkin, J. E., Levenson, N. A., & Teplitz, H. I. 2000, SPIE, 4008, 1048
- Melo, C. D. F. 2003, A&A, 410, 269
- Morbey, C. L., & Griffin, R. F. 1987, ApJ, 317, 343
- Neuhauser, R., et al. 1998, A&A, 334, 873
- Patience, J., Ghez, A. M., Reid, I. N., & Matthews, K. 2002, AJ, 123, 1570
- Petr, M. G., Coude Du Foresto, V., Beckwith, S. V. W., Richichi, A., & McCaughrean, M. J. 1998, ApJ, 500, 825
- Prato, L. 1998, Ph.D. Thesis, SUNY Stony Brook
- Prato, L., Simon, M., Mazeh, T., McLean, I. S., Norman, D., & Zucker, S. 2002a, ApJ, 569, 863
- Prato, L., Simon, M., Mazeh, T., Zucker, S., & McLean, I. S. 2002b, ApJ, 579, L99
- Ratzka, T., Köhler, R., & Leinert, Ch. 2005, A&A, 437, 611
- Reipurth, B., Lindgren, H., Mayor, M., Mermilliod, J-C., & Cramer, N. 2002, AJ, 124, 2813
- Saar, S., & Donahue, R. 1997, ApJ, 485, 319
- Siegler, N., Close, L. M., Mamajek, E. E., & Freed, M. 2003, ApJ, 598, 1265

- Siegler, N., Close, L. M., Cruz, K. L., Martín, E. L., & Reid, I. N. 2005, *ApJ*, 621, 1023
- Simon, M., et al. 1995, *ApJ*, 443, 625
- Simon, M., Dutrey, A., & Guilloteau, S. 2000, *ApJ*, 545, 1034
- Simon, M., & Prato, L. 2004, *ApJ*, 613, L69
- Stassun, K. G., Mathieu, R. D., & Valenti, J. A. 2006, *Nature*, 440, 311
- Steffen, A. T., et al. 2001, *AJ*, 122, 997
- Sterzik, M. F., Durisen, R. H., & Zinnecker, H. 2003, *A&A*, 411, 91
- Torres, G., & Ribas, I. 2002, *ApJ*, 567, 1140
- Vrba, F. J., Coyne, G. V., & Tapia, S. 1993, *AJ*, 105, 1010
- Walter, F. M., Brown, A., Mathieu, R. D., Myers, P. C., & Vrba, F. J. 1988, *AJ*, 96, 297
- Walter, F.M., Vrba, F. J., Mathieu, R. D., Brown, A., & Myers, P. C. 1994, *AJ*, 107, 692
- White, R. J., Ghez, A. M., Reid, I. N., & Schultz, G. 1999, *ApJ*, 520, 811
- Wilson, O. C. 1941, *ApJ*, 93, 29
- Zucker, S., & Mazeh, T. 1994, *ApJ*, 420, 806

Table 1. Target List

Object	α (J2000.0)	δ (J2000.0)	PMS Class	H^a (mag)	# of Obs	Sp Type	$< v_{rad} >$ (km s $^{-1}$)	$\sigma_{v_{rad}}$ (km s $^{-1}$)	Comments
						<u>Smoke Rings</u>			
RX J1612.3–1909	16 12 20.9	–19 09 05	W	9.9	4	M1	–10.52	6.30	SB1; broad lines; aka ScoPMS 51
RX J1612.6–1859	16 12 39.2	–18 59 28	C	9.5	3	M1	–5.64	0.63	ScoPMS 52, a K0, is 19.2'' E
RX J1612.6–1924Ew ^b	16 12 41.2	–19 24 18	W	9.1	3	M0	–9.49	3.22	radial velocity variable
RX J1612.6–1924Ee ^c	16 12 41.2	–19 24 18	1	M1	–11.97	...	Ew+Ee: 1'' pair ^d
RX J1613.1–1904N	16 13 10.2	–19 04 13	W	10.0	3	M2.5	–5.50	0.24	N: 0.5'' pair ^d ; spectra unresolved
RX J1613.1–1904S	16 13 10.0	–19 04 27	C	11.1	3	M4	–6.46	0.48	
RX J1613.7–1926S	16 13 43.9	–19 26 49	W	9.2	3	M0	–6.88	0.24	
RX J1613.7–1926N	16 13 43.9	–19 26 49	3	M1	–8.39	0.24	S+N: 0.7'' pair ^d
RX J1613.8–1835	16 13 47.5	–18 35 01	W	10.3	3	M1.5	–6.19	0.41	fainter, unobserved star 7.3'' N
RX J1613.9–1848	16 13 58.2	–18 48 29	W	10.1	4	M2	–6.91	0.52	
RX J1614.4–1857	16 14 28.9	–18 57 23	W	9.7	3	M2.5	–5.78	0.41	
RX J1615.1–1851	16 15 08.6	–18 51 01	W	9.9	3	M0	–4.95	0.41	
						<u>R7</u>			
RX J1621.4–2332	16 21 28.7	–23 32 49	W	10.1	3	M0.5	–7.15	0.48	brighter, unobserved star 9.7'' N ^e
RX J1622.6–2345	16 22 37.6	–23 45 51	W	10.1	3	M2	–6.46	0.48	
RX J1622.7–2325Ne	16 22 46.8	–23 25 33	W	8.7	4	M0.5	–5.78	0.75	Ne: 0.1'' pair ^d
RX J1622.7–2325Nw	16 22 46.8	–23 25 33	4	M1	SB2; Ne+Nw: 0.9'' pair ^d
RX J1622.7–2325S	16 22 47.2	–23 25 45	W	10.0	3	M0.5	–6.88	0.63	
RX J1622.8–2333	16 22 53.4	–23 33 10	W	9.9	4	K7	–3.40	4.41	SB1
RX J1622.9–2326	16 22 59.9	–23 26 35	P	9.4	3	M0	–7.29	0.24	
						<u>ρ Oph Core</u>			
RX J1624.2–2427	16 24 15.9	–24 27 35	P	9.6	3	M0	–5.91	0.48	
RX J1625.2–2455	16 25 14.7	–24 55 45	W	8.6	3	K7	–6.88	0.95	
ROXR1 3	16 25 24.3	–24 29 44	C	9.2	4	M3	–6.60	0.58	
ROXR1 7	16 25 47.7	–24 37 39	W	10.8	3	M2.5	–3.99	0.48	
ROXR1 14	16 26 03.3	–24 17 47	W	9.6	4	M1	SB2

Table 1—Continued

Object	α (J2000.0)	δ (J2000.0)	PMS Class	H^a (mag)	# of Obs	Sp Type	$\langle v_{rad} \rangle$ (km s $^{-1}$)	$\sigma_{v_{rad}}$ (km s $^{-1}$)	Comments
RX J1626.3–2407	16 26 18.8	–24 07 19	W	9.8	3	M2.5	–7.29	0.63	
ROXR1 20	16 26 19.5	–24 37 27	W	10.4	3	M4	–6.46	0.24	
ROXR1 31	16 26 44.3	–24 43 14	W	9.9	3	M1.5	–6.33	1.95 ^f	
RX J1627.6–2404W	16 27 38.3	–24 04 01	W	9.5	3	K7	–7.01 ^g	...	
ROXR1 51	16 27 39.4	–24 39 16	C	9.3	3	M0	–6.60	0.83	
RX J1627.6–2404E	16 27 41.9	–24 04 27	P	10.0	3	M2	–7.29	0.48	
RX J1628.0–2448	16 28 00.0	–24 48 19	W	9.8	2	M2	–9.49 ^g	...	broad lines
<u>Streamers</u>									
RX J1632.7–2332	16 32 44.4	–23 32 13	P	10.9	3	M2.5	–9.63	0.24	
RX J1636.2–2420	16 36 16.9	–24 20 34	P	10.3	3	M3	–2.06 ^g	...	

Note. — The best coordinates were defined using *2MASS* positions of the targets. In most cases these were consistent with SIMBAD, however, for about 20% of the targets, the SIMBAD coordinates were off by 6'' or more.

^a H magnitudes from *2MASS*; for the three sub-arcsecond visual binaries with both components listed the total systemic magnitude is given with the entry for the primary.

^bSIMBAD coordinates for the Ew-Ee pair point to an object with a featureless spectrum 17.2'' to the west.

^cThe eastern component in this 1'' pair was only observed once but has a velocity that is distinct from the local mean; it should be reobserved for variability.

^dThis work.

^eVrba et al. (1993) classify this object, VSS II-137, as an F star.

^fRadial velocity scatter probably attributable to poor SNR, 60, in one spectrum vs. 200 in the others, but should be reobserved.

^gAll radial velocity measurements equal.

Table 2. Spectral Type Standards

Object Name	Spectral Type from literature	Reference	Spectral Type determined here
GJ 763	M0	1	M0
GJ 752A	M3	1	M2
GJ 436	M3	1	M2.5
GJ 15A	M1.5	2	M3
GJ 402	M4	1	M4

References. — (1) Kirkpatrick et al. (1991); (2) Henry et al. (1994).

Table 3. Spectroscopic Binary Component Velocities

BJD ^a (2,450,000+)	v_1^b (km s ⁻¹)	v_2^b (km s ⁻¹)
<u>RX J1612.3–1909</u>		
2362.99	–14.44	...
2447.76	–2.06	...
2723.01	–9.49	...
2773.86	–16.09	...
<u>RX J1612.6–1924Ew^c</u>		
2723.06	–13.20	...
2773.99	–7.43	...
3150.86	–7.84	...
<u>RX J1622.7–2325Nw, q=0.94±0.03, $\gamma = -6.21 \pm 0.82$ km s⁻¹</u>		
2449.80	–6.19	–6.19
2771.99	44.98	–61.90
2804.94	44.56	–60.66
3198.79	31.77	–47.87
<u>RX J1622.8–2333</u>		
2473.82	–9.49	...
2724.06	–0.41	...
2804.97	–0.83	...
3199.79	–3.71	...
<u>ROXR1 14, q=0.98±0.02, $\gamma = -6.16 \pm 0.43$ km s⁻¹</u>		
2363.16	–6.19	–6.19
2449.90	34.25	–47.45
2773.89	–42.50	30.95
3124.97	33.01	–46.22

^aBarycentric Julian date.

^bSystematic uncertainties are ~ 1 km s⁻¹.

^cRadial velocity variable; see Table 1 and §4.3.2.

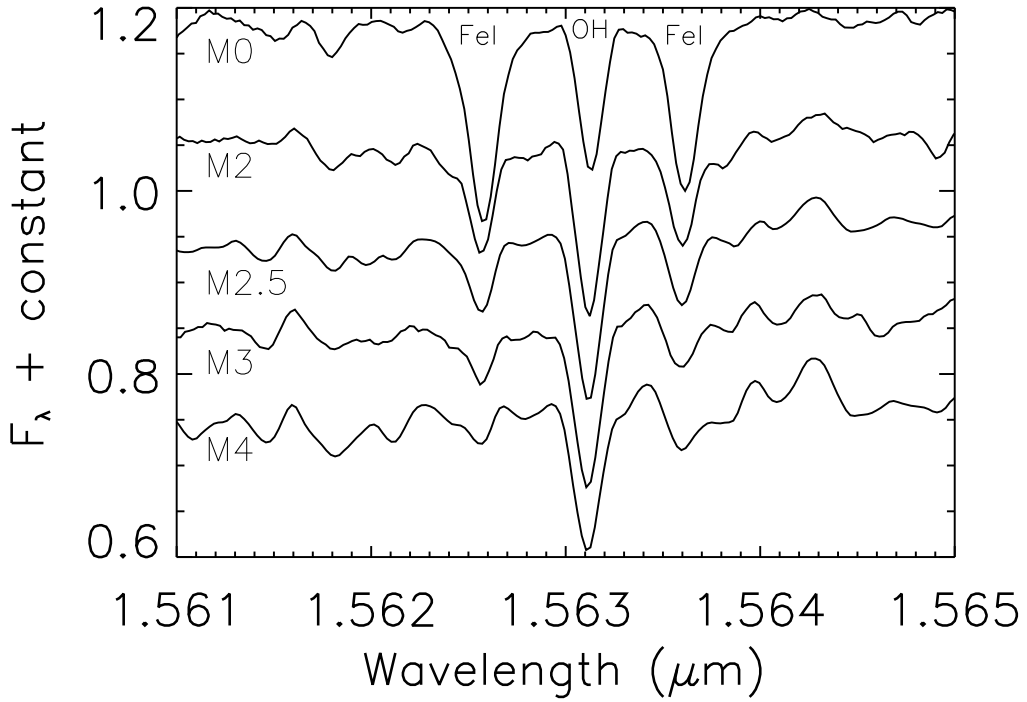


Fig. 1.— Spectral type standard star sequence, as determined from high-resolution H -band spectra. See Table 2 for spectral types identified in the literature. All spectra are presented on a heliocentric wavelength scale and all have been rotationally broadened to $v \sin i \sim 15 \text{ km s}^{-1}$, close to the average $v \sin i$ for the sample.

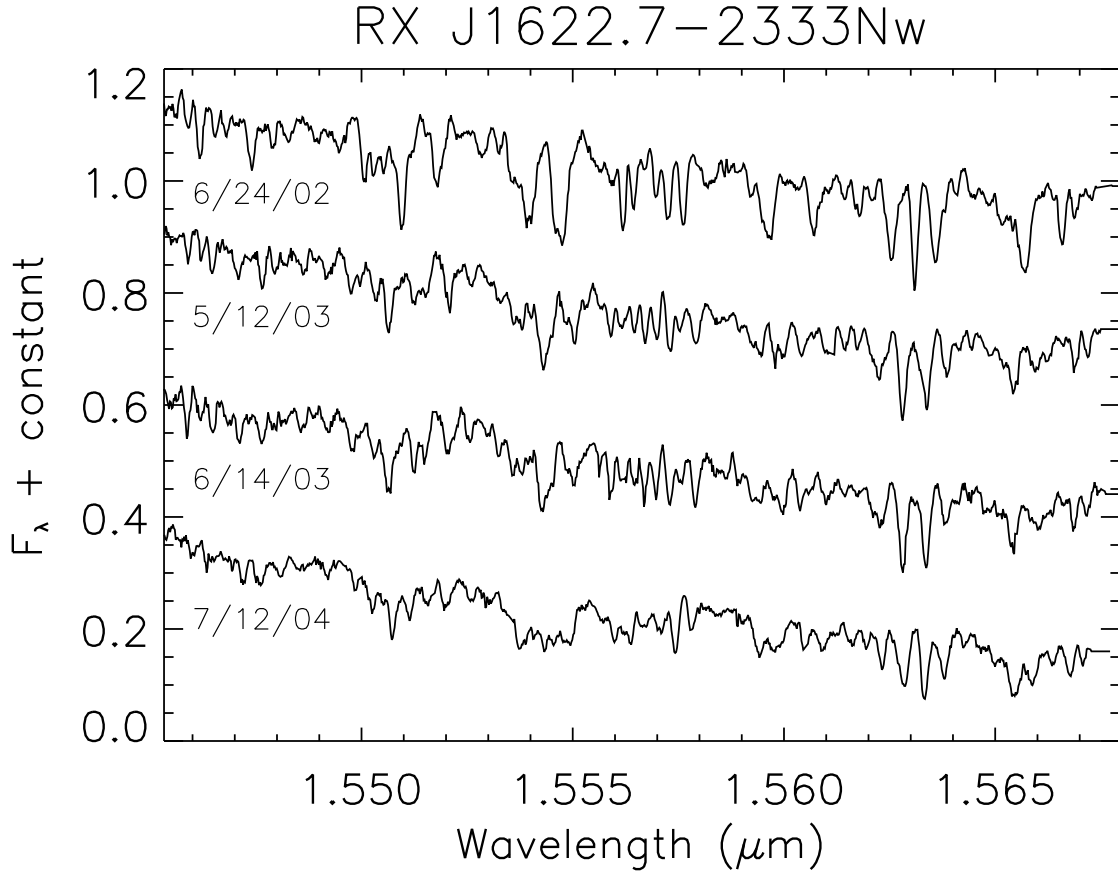


Fig. 2.— Four epochs of spectra for the SB2 RX J1622.7–2325Nw; UT dates of the observations are indicated.

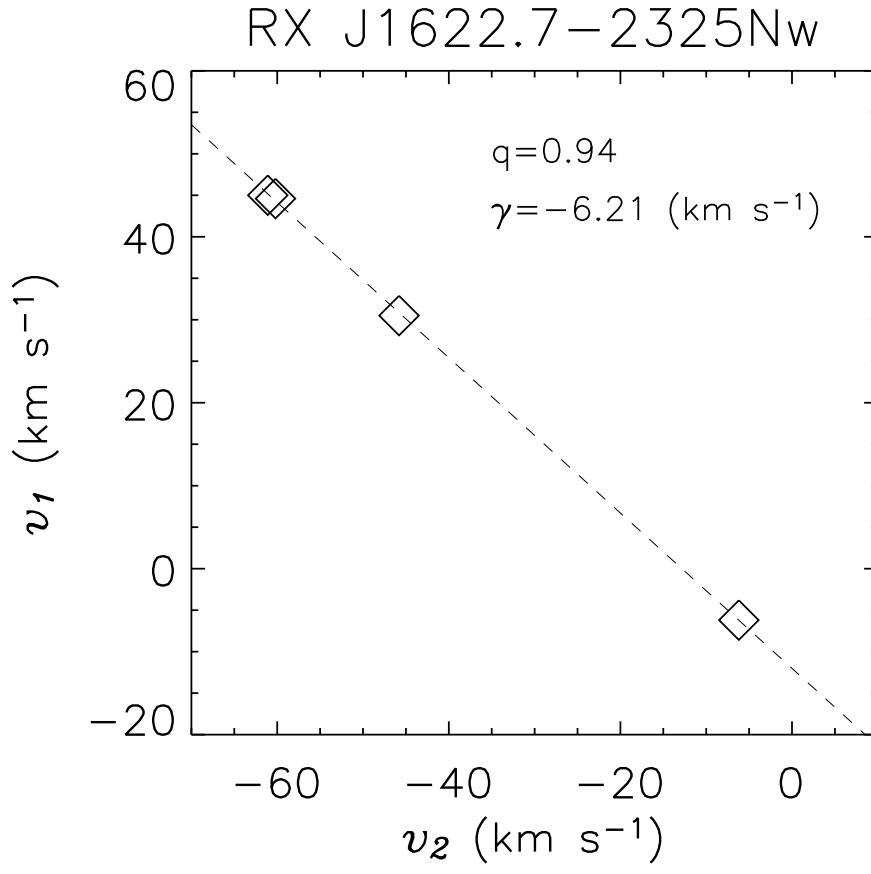


Fig. 3.— Linear fit to the primary versus secondary radial velocities for RX J1622.7–2325Nw.

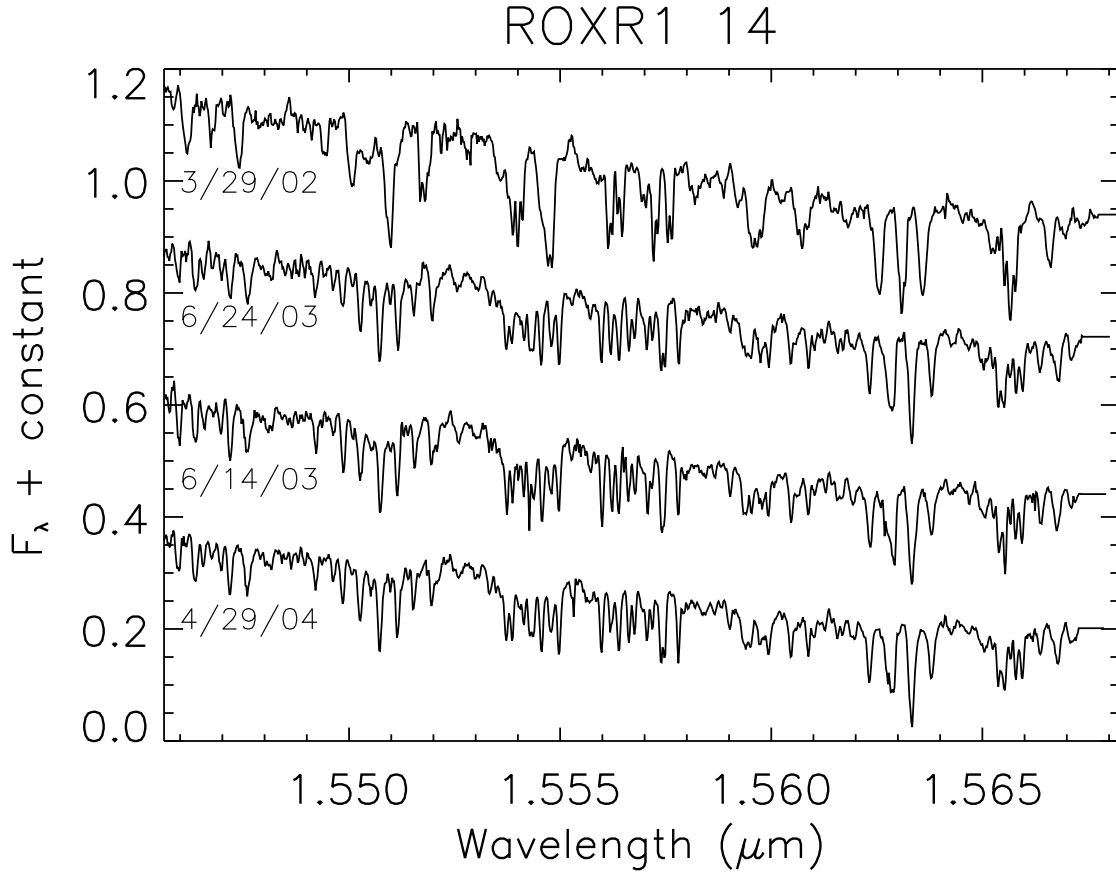


Fig. 4.— Four epochs of spectra for the SB2 ROXR1 14; UT dates of the observations are indicated.

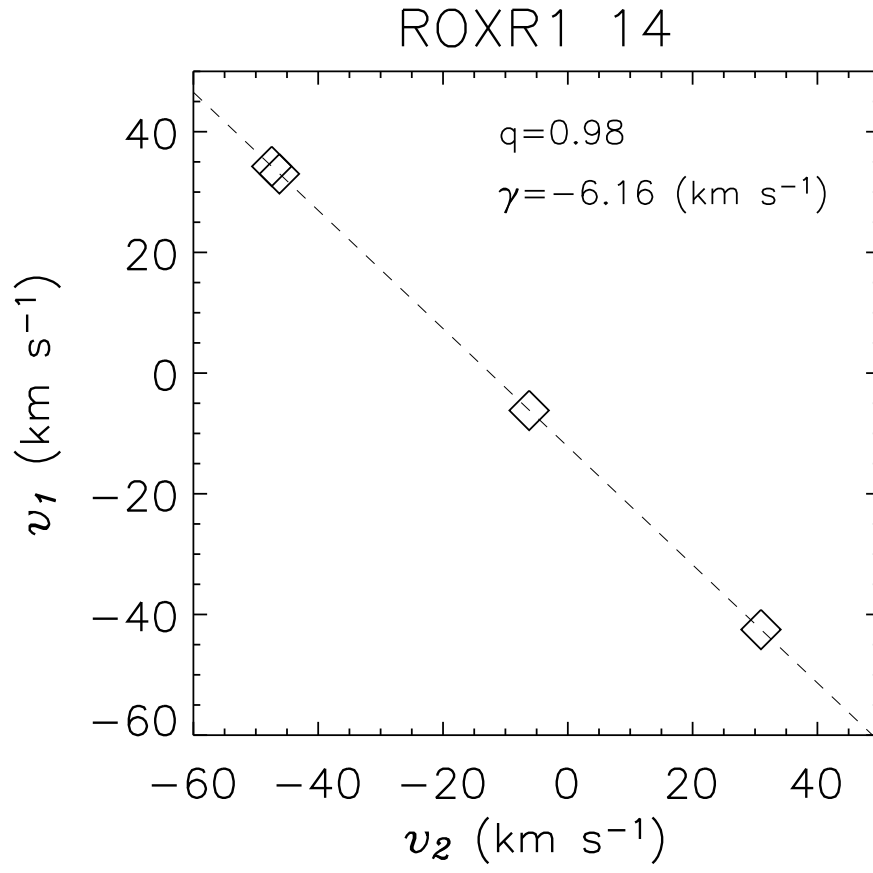


Fig. 5.— Linear fit to the primary versus secondary radial velocities for ROXR1 14.

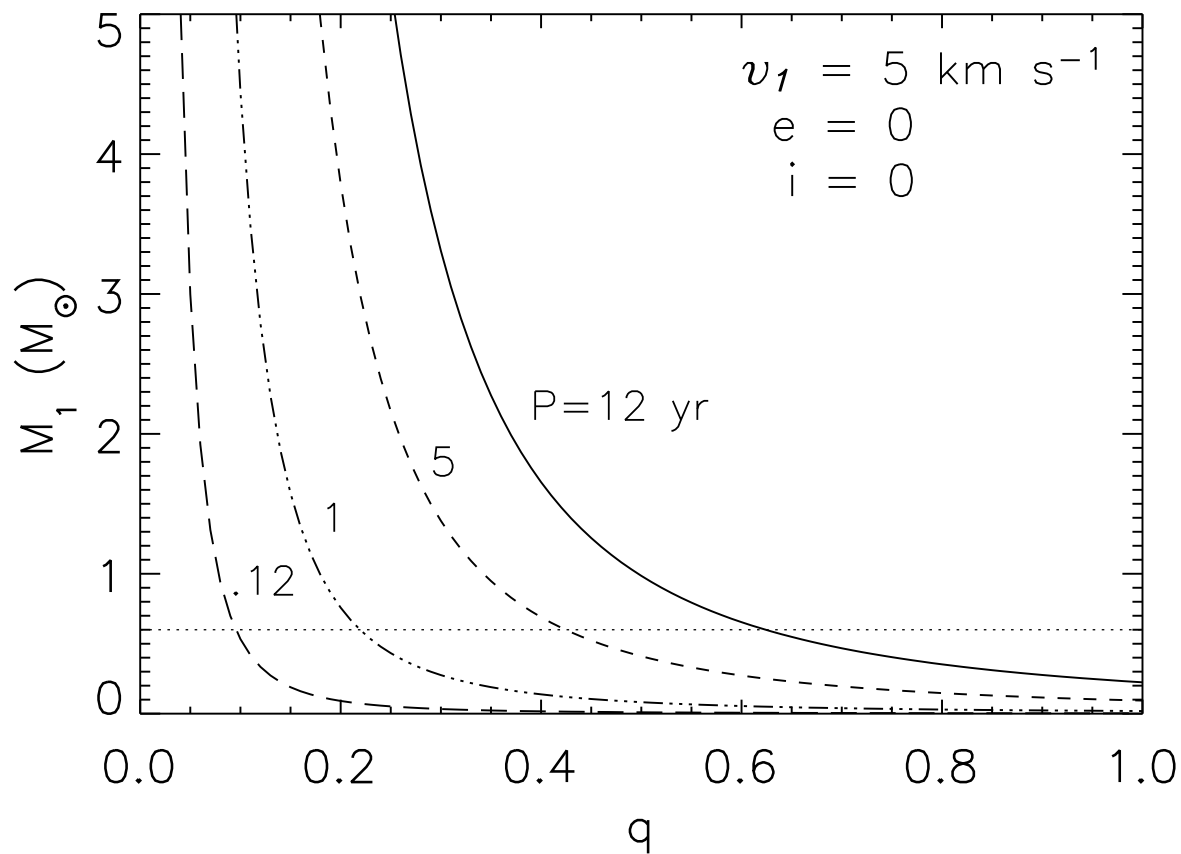


Fig. 6.— Primary star mass as a function of mass ratio, q , for a range of orbital periods from 0.12 to 12 years and a primary star velocity of 5 km s^{-1} . Assumes circular, edge-on orbits. To detect a mass ratio of 0.1 in a system with a primary star mass of $0.6 M_\odot$, implying a substellar mass companion (dotted line), requires a period of less than 0.11 years, or ~ 40 days.